Nup98 regulates bipolar spindle assembly through association with microtubules and opposition of MCAK

Marie K. Cross[a,b] and Maureen A. Powers[a]
[a]Department of Cell Biology and [b]Biochemistry, Cell, and Developmental Biology Graduate Program, Emory University School of Medicine, Atlanta, GA 30322

ABSTRACT During mitosis, the nuclear pore complex is disassembled and, increasingly, nucleoporins are proving to have mitotic functions when released from the pore. We find a contribution of the nucleoporin Nup98 to mitotic spindle assembly through regulation of microtubule dynamics. When added to *Xenopus* extract spindle assembly assays, the C-terminal domain of Nup98 stimulates uncontrolled growth of microtubules. Conversely, inhibition or depletion of Nup98 leads to formation of stable monopolar spindles. Spindle bipolarity is restored by addition of purified, recombinant Nup98 C-terminus. The minimal required region of Nup98 corresponds to a portion of the C-terminal domain lacking a previously characterized function. We show association between this region of the C-terminus of Nup98 and both Taxol-stabilized microtubules and the microtubule-depolymerizing mitotic centromere–associated kinesin (MCAK). Importantly, we demonstrate that this domain of Nup98 inhibits MCAK depolymerization activity in vitro. These data support a model in which Nup98 interacts with microtubules and antagonizes MCAK activity, thus promoting bipolar spindle assembly.

INTRODUCTION

The nuclear pore complex (NPC) is a large multiprotein structure that functions as a gateway for regulated movement of macromolecules between the nucleus and cytoplasm (reviewed in Tran and Wente, 2006; D'Angelo and Hetzer, 2008). The NPC is made up of roughly 30 different proteins termed nucleoporins, or Nups, one-third of which contain a domain with multiple, interspersed copies of the peptide repeat phenylalanine–glycine (FG) (Schwartz, 2005;

Devos *et al.*, 2006). The FG-repeat domains of nucleoporins are thought to be relatively unstructured regions that associate with one another largely through hydrophobic interactions. Nuclear transport receptors such as importin β and other karyopherin family members are capable of regulated interaction with FG domains in order to selectively import and export proteins and RNA (reviewed in Terry *et al.*, 2007). The meshwork of FG domains also provides a barrier to nonspecific diffusion of macromolecules while allowing free passage of smaller proteins and molecules. Thus NPCs play a critical role in the maintenance of correct cellular compartmentalization.

During mitosis in metazoan cells, the nuclear envelope breaks down and nuclear pores disassemble into conserved nucleoporin subcomplexes (Rabut *et al.*, 2004). With the exception of transmembrane nucleoporins, these complexes are soluble and are generally dispersed throughout the dividing cell. Until recently, such mitotic nucleoporin subcomplexes were thought to remain dormant until the nuclear envelope and NPC began to reform in telophase. Unexpectedly, it has developed that, in addition to the established mitotic role of nuclear transport receptors, nucleoporins also make functional contributions to mitosis, although in many cases the underlying mechanisms remain unclear (Roux and Burke, 2006; Kutay and Hetzer, 2008).

The nuclear import factors importin α and importin β are responsible for sequestering various spindle components during mitosis

and delivering them appropriately in the vicinity of mitotic chromatin (reviewed in Clarke and Zhang, 2008; Kalab and Heald, 2008). The GTPase Ran directs the localized release of assembly factors from importins. This is accomplished by RCC1, the Ran guanine nucleotide exchange factor (GEF), which is bound to chromatin and generates a Ran–guanosine 5′-triphosphate (GTP) concentration gradient. As in nuclear import, interaction with Ran-GTP induces release of bound cargo from importins. This ensures that potent mediators of spindle assembly are enriched within the appropriate area around chromatin. The importin α/importin β complex is responsible for correct localization of a variety of microtubule-associated spindle assembly factors (SAFs) including TPX2, NuMA, Xnf7, and NuSAP (Gruss et al., 2001; Nachury et al., 2001; Wiese et al., 2001; Raemaekers et al., 2003; Maresca et al., 2005). Importin β can directly bind and regulate additional factors, including HURP, Maskin, and Rae1 (Blower et al., 2005; O'Brien et al., 2005; Koffa et al., 2006). The nuclear export factor Crm1/Exportin1, which remains bound to cargo in the presence of Ran-GTP, is responsible for targeting both the Nup358/RanGAP complex and the chromosomal passenger complex (CPC) to the centromere/kinetochore region of the spindle (Arnaoutov and Dasso, 2005; Knauer et al., 2006).

A still growing list of nucleoporins plays roles in mitotic spindle assembly or in mitotic checkpoints. A fraction of both the Nup107/ELYS and Nup358/RanGAP subcomplexes are localized to mitotic kinetochores, where they contribute to formation and/or stabilization of microtubule-kinetochore attachments (Belgareh et al., 2001; Joseph et al., 2002, 2004; Salina et al., 2003; Loiodice et al., 2004; Arnaoutov and Dasso, 2005; Orjalo et al., 2006; Rasala et al., 2006; Franz et al., 2007; Zuccolo et al., 2007). Independently, ELYS and Nup153 function in cytokinesis through poorly defined activities (Rasala et al., 2006; Mackay et al., 2009). Rae1 makes multiple contributions through roles in spindle assembly and regulation of the anaphase-promoting complex/cyclosome (APC/C) and is required for a fully functional mitotic checkpoint (Whalen et al., 1997; Blower et al., 2005; Jeganathan et al., 2005; Wong et al., 2006). As well, Tpr and Nup153 contribute to targeting Mad1/2 to the kinetochore and are involved in the mitotic checkpoint (Lee et al., 2008; Lussi et al., 2010). Although this list of mitotically active nucleoporins continues to grow, the mechanisms underlying their roles are incompletely understood. One exception is the recent elegant demonstration that the Nup107 complex promotes microtubule nucleation at kinetochores through interaction with the γ-tubulin ring complex (γ-TuRC) (Mishra et al., 2010). This complex was also shown by others to interact with the CPC at the mitotic kinetochore (Platani et al., 2009).

Here we report that the nucleoporin Nup98 functions in mitotic spindle assembly by influencing microtubule dynamics. Nup98 is a glycine-leucine-phenylalanine-glycine (GLFG) repeat containing nucleoporin dynamically associated with both nuclear and cytoplasmic faces of the NPC (Radu et al., 1995; Griffis et al., 2002, 2003). During interphase, Nup98 participates in RNA export and protein import (Powers et al., 1997; Fontoura et al., 2000). A fraction of Nup98 is found within the nuclear interior (Powers et al., 1995) and very recently was shown to function in regulation of genes contributing to cell cycle and development (Capelson et al., 2010; Kalverda et al., 2010). During mitosis, Nup98 is soluble and largely dispersed throughout the cell. We found that addition of the Nup98 C-terminal domain to Xenopus spindle assembly assays caused excess tubulin polymerization and highly disordered bipolar spindles. In contrast, inhibition of Nup98 in the egg extract led to accumulation of monopolar spindles. Importantly, addition of recombinant Nup98 C-terminus restored spindle bipolarity in depleted extracts. We have mapped the specific region of Nup98 involved and established

that its function is independent of the Nup107 complex, a Nup98 binding partner in the NPC. We propose a model in which Nup98 regulates plus-end microtubule dynamics, and, in support of this model, we show that the relevant region of Nup98 interacts with Taxol-stabilized microtubules and inhibits the depolymerizing mitotic centromere–associated kinesin (MCAK), a major regulator of microtubule dynamics in the spindle.

RESULTS

Addition of purified Nup98 C-terminal domain to CSF extract disrupts spindle assembly

To investigate the potential mitotic function of Nup98, we added a bacterially expressed Nup98 C-terminal fragment (His-tagged amino acids [aa] 506–920; Supplemental Figure 1) to Xenopus laevis spindle assembly assays in vitro. The purified fragment was added to Xenopus cytostatic factor (CSF) egg extracts to a final concentration of 6 µM along with sperm chromatin, and, at time points during spindle assembly, samples were fixed and analyzed by fluorescence microscopy. As expected, after 15 min, microtubule asters had formed in control samples (Figure 1Aa). Surprisingly, in the presence of the Nup98 C-terminal fragment, asters contained longer microtubules (Figure 1Ab). This microtubule phenotype persisted throughout the time course of spindle formation and resulted in highly perturbed bipolar spindle structures. In contrast, spindles formed in the presence of the same concentration of a control protein (bovine serum albumin [BSA]) displayed normal bipolar spindle morphology (Figure 1A, compare panels i and m to panels j and n). Protein obtained by purification of control bacterial lysate over a nickel chromatography column had no effect when added to the spindle assembly assay (unpublished data).

To demonstrate independently and quantitatively that this Nup98-induced phenotype represented excess microtubule growth, we used a tubulin spin-down assay. Following formation of spindles in the presence or absence of the Nup98 C-terminal domain, tubulin polymers were separated from unincorporated tubulin by pelleting through a glycerol cushion and then immunoblotted to compare amounts of polymerized tubulin (Figure 1B, left). Both γ-tubulin and RCC1, the chromatin-binding Ran GEF protein, were used as loading controls and gave similar results (Figure 1B, right). These assays confirmed that in the presence of the Nup98 C-terminal domain there is indeed an increased amount of tubulin polymerization.

In cycled Xenopus extracts, the CSF extract is first shifted into interphase, allowing nuclei to assemble and replicate both chromatin and centrosomes. The nuclei are then cycled back into mitosis by addition of fresh CSF extract, and bipolar spindles form. When the Nup98 fragment was added to cycled extracts, spindles showed excess microtubule polymerization and a disrupted spindle structure, exactly as seen with noncycled spindles (Supplemental Figure 2A).

The Nup98 fragment used in these assays includes the domain responsible for autoproteolytic cleavage of Nup98 at residue F863 (Rosenblum and Blobel, 1999). This domain is additionally involved in targeting Nup98 to the NPC through interaction primarily with Nup96 within the Nup107 complex, but also with Nup88 (Hodel et al., 2002; Griffis et al., 2003). To determine whether this same domain was sufficient for the observed effect on spindle assembly, a shorter fragment of the Nup98 C-terminus (aa 678–920), corresponding to the autoproteolytic and minimal NPC-targeting domain, was tested. Following addition of this shorter fragment to the assays, normal bipolar spindles formed that were indistinguishable from controls (Figure 1A, panels c, g, k, and o). Therefore we conclude that a region between residues 506 and 677 of Nup98 is required for the excess microtubule phenotype.
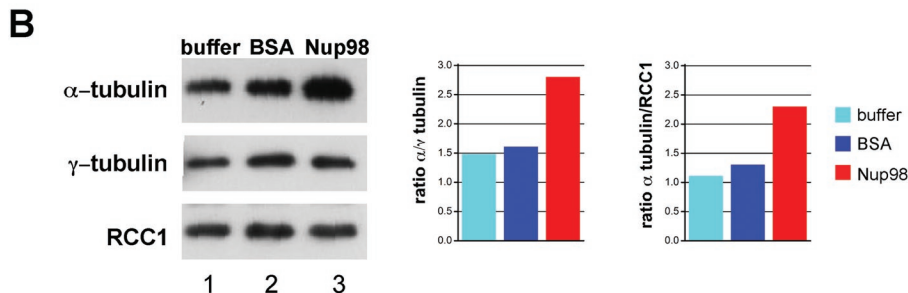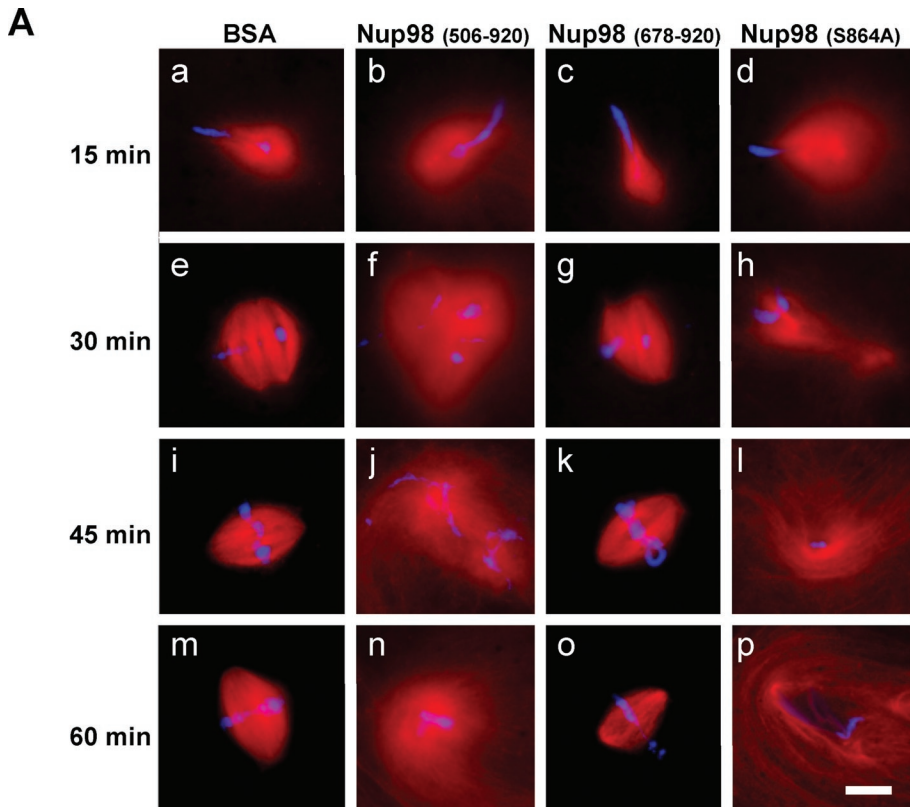
FIGURE 1: A C-terminal domain fragment of Nup98 causes excess microtubule polymerization during assembly of meiotic spindles. (A) Nup98 C-terminal domain fragments or BSA were added at 6 μM at the start of assembly assays. The excess microtubule phenotype could be observed at concentrations as low as 2.5 μM; by immunoblotting, we estimate the endogenous Nup98 concentration at ~0.6 μM in the extract. Samples were examined at the indicated time points. Microtubules are labeled with X-rhodamine tubulin (red), and DNA is labeled with Hoechst (blue). Scale bar represents 20 μm. (B) Left, polymerized tubulin was isolated and immunoblotted for α-tubulin. Both γ-tubulin and RCC1 were blotted as loading controls. Right, quantitation of tubulin polymerization using either γ-tubulin (left) or RCC1 (right) for normalization.

The Nup107 complex, composed of Nups107, 160, 133, 96, 85, 43, 37, Sec13, and Seh1, has been shown to play a role in assembly of a correct bipolar spindle in *Xenopus* mitotic extract (Orjalo *et al.*, 2006). A fraction of this complex is physically associated with the mitotic kinetochore, where it was recently shown to recruit γ-TuRC to the kinetochore and promote Ran-dependent microtubule polymerization (Belgareh *et al.*, 2001; Zuccolo *et al.*, 2007; Mishra *et al.*, 2010). Given that one member of this complex, Nup96, is a binding partner of the Nup98 C-terminal domain (Vasu *et al.*, 2001; Hodel *et al.*, 2002), we asked whether interaction between Nup98 and the Nup107 complex underlies the Nup98 C-terminal phenotype. We tested two constructs: first, a mutant unable to undergo autocatalytic cleavage (S864A) and thus unable to bind Nup96 (Hodel *et al.*, 2002), and, second, a mutant truncated at the autocatalytic site (F863), which removes the short stretch of amino acids beyond the cleavage site that is identical to the Nup96 N-terminus. Both of these mutant constructs induced excess microtubule polymerization during spindle assembly (Figure 1A and Supplemental Figure 1). Thus the unregulated microtubule polymerization phenotype is a novel function of Nup98 and independent of Nup96 and the Nup107 complex.

Nup98 and alternative spindle assembly pathways

There are multiple distinct pathways that can work in conjunction to build a mitotic spindle (O'Connell and Khodjakov, 2007; Kalab and Heald, 2008; Walczak and Heald, 2008). In cultured cells, the predominant pathway is thought to be the centrosome-driven or search-and-capture pathway, in which microtubules extend dynamically from the centrosome and search for the kinetochore complex found on the centromeric region of the chromosome. However, there is also a second, chromatin-driven pathway, regulated by the Ran GTPase, in which microtubules polymerize adjacent to chromatin and are then organized by molecular motors and other factors to form a spindle pole. The chromatin-driven pathway is thought to be the major spindle assembly pathway in *Xenopus* egg extracts. Spindle-like Ran asters form in CSF extract upon addition of a nonhydrolyzing variant of Ran-GTP, even in the absence of centrosomes (Carazo-Salas *et al.*, 1999; Kalab *et al.*, 1999; Ohba *et al.*, 1999; Wilde and Zheng, 1999; Zhang *et al.*, 1999). We found that addition of purified Nup98 C-terminus to Ran aster assays led to excess polymerization of microtubules (Figure 2A). Asters were larger, with more unfocused microtubules. This result was confirmed biochemically by the tubulin spin-down assay (Figure 2A).

Importantly, we found that when purified Nup98 C-terminal domain was added to *Xenopus* egg extract in the absence
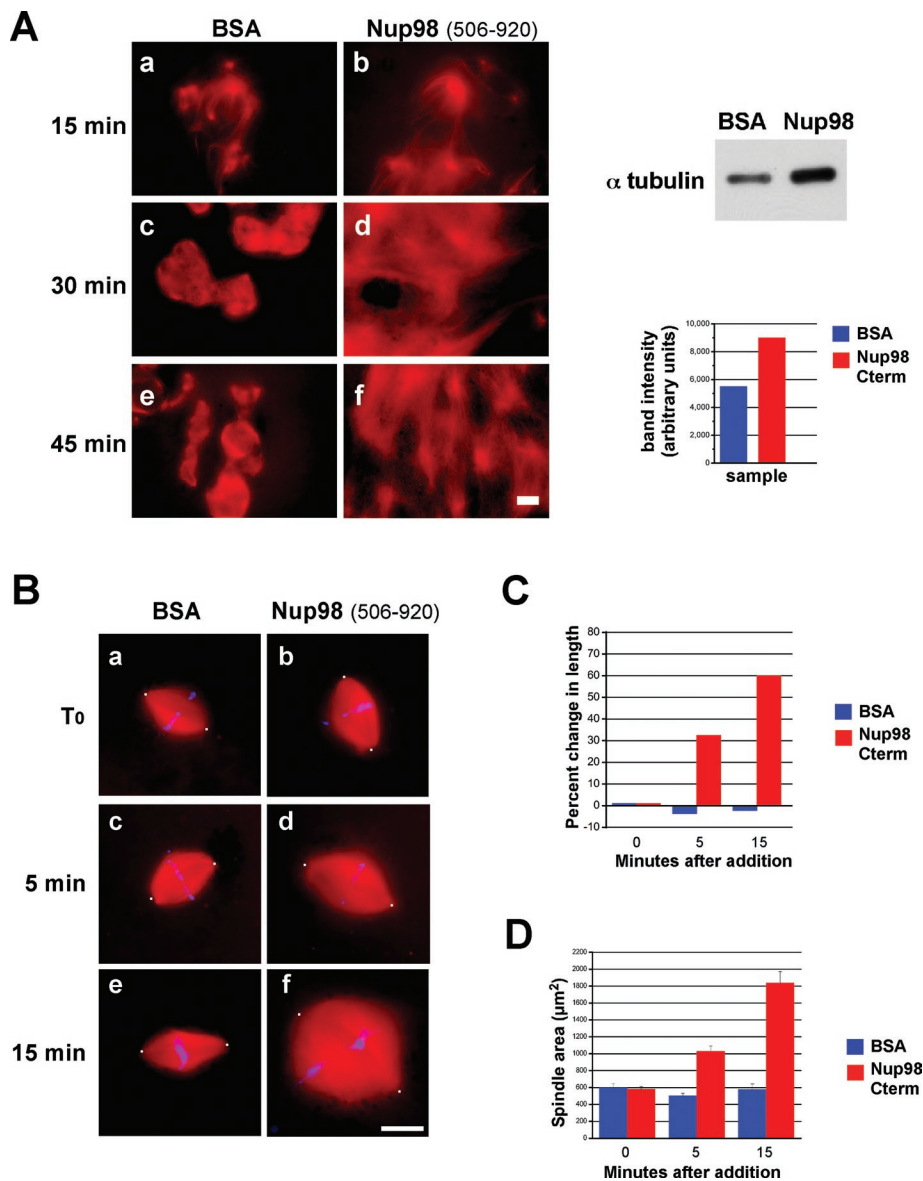
Further deletion analysis was carried out to identify a region sufficient for this effect (Supplemental Figure 1). Samples were scored for the presence or absence of the excess microtubule phenotype; additionally, spindle size was quantified as a measure of the extent of the phenotype. The minimal fragment of Nup98 required for the microtubule phenotype was determined to be aa 506–774. Interestingly, no function has been previously defined for the region between aa 506 and 710; the remainder of the minimal fragment, aa 711–774, corresponds to the first half of the autoproteolytic domain. Because this minimal fragment proved to be less stable upon storage following purification, we continued to use the full C-terminal fragment for most subsequent experiments.

FIGURE 2: The Nup98 C-terminal domain increases microtubule polymerization in Ran asters and in preformed spindles. (A) Left, Nup98 C-terminus or BSA was added along with 25 µM RanQ69L to *Xenopus* extract, and Ran aster formation was monitored. Microtubules are labeled with X-rhodamine tubulin (red). Scale bar is 20 µm. Right, Ran asters formed in the presence or absence of the Nup98 C-terminus were assayed by tubulin spin-down. (B) Spindles were preformed in *Xenopus* egg extract for 60 min. Either BSA or Nup98 C-terminus was then added (T0), and spindles were monitored over time. Scale bar is 20 µm. (C) Spindle length was measured as pole-to-pole distance (indicated by white dots). Percentage of change was calculated as (average spindle length in sample) – (average T0 length) / (average T0 length) × 100. An average of 10 spindles was quantified for each point except the 15-min Nup98 sample, in which only 6 intact spindles could be identified. (D) Average spindle area in µm² for each time point was measured using MetaMorph.

fects of the Nup98 fragment? To assess this, we preformed spindles in CSF extract, divided the sample into two parts, and added either BSA or the Nup98 C-terminus. Strikingly, within 5 min after addition of the Nup98 fragment, the spindles began to elongate from pole to pole (Figure 2B). By 15 min after addition, while control spindles remained unchanged, the structure of the spindles in the presence of the C-terminal domain of Nup98 was greatly altered due to the increase in microtubule growth. By 30 min, spindles were highly distorted and disrupted in structure. These effects were quantified by measuring the percentage of change in spindle length (Figure 2C) and the change in spindle area (Figure 2D). Similar results were obtained using cycled spindles (Supplemental Figure 2B). Taken together, our data indicate that Nup98 does not initiate microtubule polymerization but can influence microtubule growth regardless of the pathway through which polymerization is initiated.

Nup98 antibodies inhibit formation of bipolar spindles but do not affect Ran asters or preformed spindles

To this point, experiments had been conducted by the addition of exogenous, recombinant Nup98 fragments to the extract. To test for a contribution from endogenous Nup98 in spindle assembly, we first added Nup98-specific antibodies to block endogenous protein function. If the Nup98 C-terminal fragment competed for binding of a factor to endogenous Nup98, we hypothesized that an antibody binding this same region of endogenous Nup98 might phenocopy the effect of the fragment. However, in contrast to excess tubulin polymerization, the addition of antibody raised against either *Xenopus* or human Nup98 C-terminal domain led to a reduction in bipolar spindles and a corresponding increase in monopolar spindles up to >50% monopoles (Figure 3, A and B). Control assays in which the antibody was preabsorbed with the Nup98 fragment showed no effect of antibody addition (unpublished data), demonstrating that the inhibition was due to specific Nup98 binding. We measured the size of each spindle type in these assays and

of either sperm chromatin or Ran-GTP, it is unable to independently initiate microtubule polymerization (unpublished data). Therefore the excess microtubule phenotype is not due to direct initiation of microtubule polymers by Nup98. Rather, addition of the C-terminal domain of Nup98 is affecting the dynamics of microtubules once polymerization is initiated by other factors.

The Nup98 fragment clearly perturbed formation of spindles, but would an existing normal bipolar spindle still be sensitive to ef-

found no significant differences in size (Supplemental Figure 4A). Independent immunoblot and immunofluorescence studies revealed that the human Nup98 C-terminal antibody is directed almost entirely toward epitopes within aa 506–677 (S. Xu and M. Powers, unpublished data); there is only minimal recognition of the region from aa 678–920, most likely due to the high structural conservation of the autoproteolytic domain (Robinson *et al.*, 2005). This antibody thus proved to be an ideal reagent for inhibition of this Nup98 function.
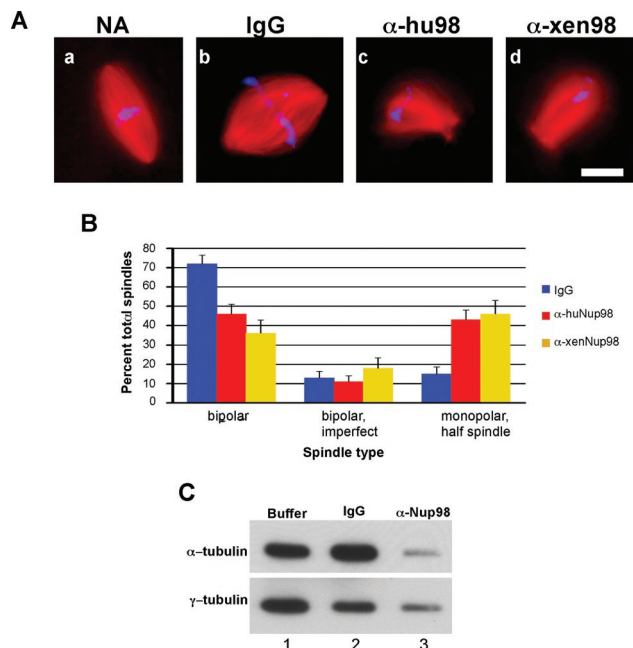
FIGURE 3: Addition of Nup98-specific antibodies causes a shift to monopolar spindles. (A) Antibodies raised to either human or *Xenopus* Nup98 were added to spindle assays at 200 or 100 µg/ml, respectively. Nonspecific rabbit IgG was added at 200 µg/ml. Assays were incubated for 60 min. Microtubules are in red; DNA is in blue. Scale bar is 20 µm. (B) Spindle morphology was quantified with spindles scored as either bipolar, imperfect bipolar, or monopolar; 25–50 spindles were scored for each condition in three independent experiments for a total of 250 spindles. Error bars represent standard error of the proportion (SEP). (C) Polymerized tubulin was pelleted and analyzed by immunoblotting. The smaller half-spindles formed in Nup98 samples pelleted less efficiently, leading to decreases in both α- and γ-tubulin.

In a tubulin spin-down assay, we observed a substantial reduction in polymerized tubulin in samples containing Nup98 antibody (Figure 3C). We noted that the level of γ-tubulin was also reduced (Figure 3C, lane 3), which may result from the lack of a second spindle pole and/or a lessened ability of the small half-spindles to be recovered through the glycerol cushion. Once again, results of antibody addition were consistent in cycled spindle assays, with a reduction of bipolar spindles and a significant increase in monopolar spindles (Supplemental Figure 2A). The opposing phenotypes obtained from addition of the Nup98 C-terminus and addition of Nup98 C-terminal antibodies indicated that, rather than acting as a competitive inhibitor, the C-terminal domain of Nup98 contains a functional activity that promotes microtubule growth.

The C-terminal antibodies were then tested in the Ran aster and preformed spindle assays. Although we had observed that addition of antibodies significantly affected bipolar spindle assembly, this same treatment had only minimal affect on Ran aster formation or on the structure of preformed spindles (unpublished data; summarized in Figure 4D). These data, taken together with the Nup98 fragment addition data, suggest that although the C-terminal domain can have a dominant effect on microtubules in spindle assembly, Ran asters, and preformed spindles, Nup98 is not essential for the Ran pathway of spindle assembly. Additionally, Nup98 is not required to maintain bipolar spindle structure once formed, although the possibility exists that, in the pre-
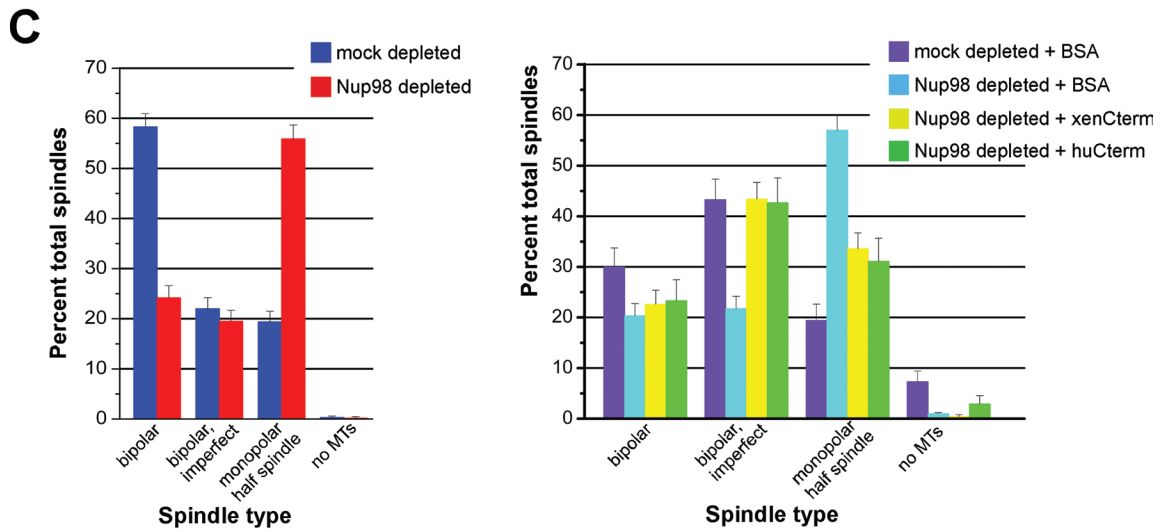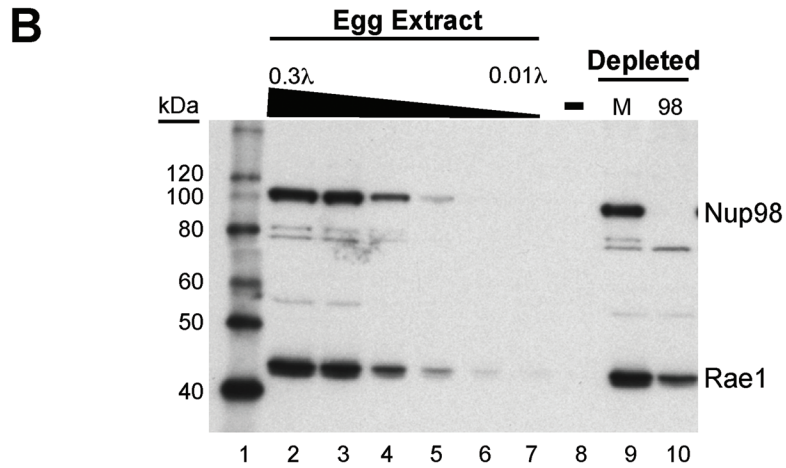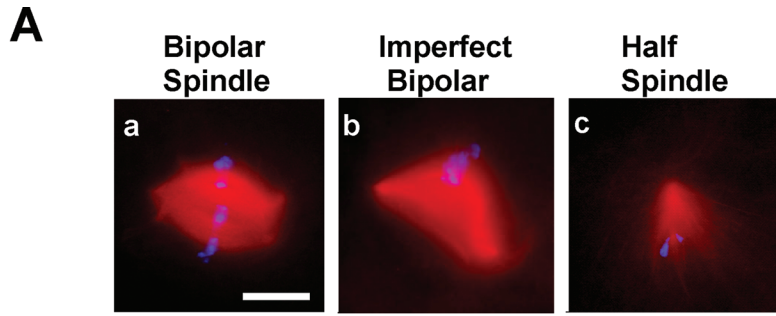
formed spindle, the Nup98 epitopes are not accessible for antibody binding.

Endogenous Nup98 is required for bipolar spindle assembly in egg extract

To address more directly the requirement for endogenous Nup98 in spindle assembly, we immunodepleted Nup98 from *Xenopus* CSF extract. Similar to Nup98 antibody addition, depletion of Nup98 before spindle assembly led to a significant decrease in bipolar spindles from ~60% to 25%, with a corresponding increase in stable monopolar spindles from ~20% to 55% (Figure 4, A and C, left). Depletion of endogenous Nup98 was confirmed by immunoblot, which indicated a greater than 90% reduction in Nup98 protein level (Figure 4B). Interestingly, analysis of the Nup98-depleted extract revealed that the Nup98 binding partner, Rae1, was only ~50% codepleted, suggesting that, in these mitotic *Xenopus* egg extracts, Nup98 is not always found in a complex with Rae1 (Figure 4B). In support of this we observed that the level of another Rae1-interacting protein was not reduced in Nup98-depleted extracts (Supplemental Figure 3).

If this region of the Nup98 C-terminus truly stimulates microtubule polymerization, we predicted that the recombinant C-terminal fragment should compensate for the loss of endogenous Nup98. Therefore we tested whether the Nup98 C-terminus could restore bipolar spindle formation to Nup98-depleted extracts. Strikingly, whereas the Nup98-depleted extract supplemented with BSA contained ~55% monopolar spindles as expected, addition of either human or *Xenopus* Nup98 C-terminus rescued spindle bipolarity to near control levels (Figure 4, A and C, right). Despite their bipolarity, many of the rescued bipolar spindles were classified as "imperfect" for reasons such as misaligned chromatin, split poles, or slightly misshapen structure (Figure 4Ab). However, the fraction of imperfect bipolar spindles obtained upon addback of Nup98 C-terminus was virtually identical to that observed in the corresponding control (Figure 4C, right; mock depletion + BSA). This observation indicates that the spindle imperfections result from dilution of the already fragile depleted extract during addback of protein. In comparing the size of different spindle types, the minimal changes we observed in monopoles were restored by addback of Nup98 C-terminus (Supplemental Figure 4B). Overall, the finding that bipolarity is restored provides strong support for our conclusion that the C-terminus of Nup98 is responsible for a function of Nup98 in bipolar spindle assembly.

Similar to Ran asters formed in the presence of Nup98 C-terminal antibodies, Ran asters formed in Nup98-depleted extract are largely unaffected (unpublished data, summarized in Figure 4D). In some extracts, we observed a minor delay of ~15 min in formation of the Ran asters when endogenous Nup98 was depleted. However, once the Ran asters formed, their structure was equivalent to Ran asters formed in control extract. This provides further evidence that Nup98 is not required for the Ran pathway of spindle formation. Taken together, our data indicate that Nup98 is critical for bipolarity of spindles but not Ran asters. Once a bipolar spindle is formed, Nup98 is no longer essential for maintenance. However, the target of Nup98 regulation is present in bipolar spindles, and excess microtubule polymerization can be stimulated by exogenous Nup98 C-terminus. Similarly, Nup98 is not required for the Ran pathway to produce the spindle-like Ran asters; however, the responsive factor is present and can be hyperactivated by addition of the Nup98 C-terminus.

A

Bipolar Spindle | Imperfect Bipolar | Half Spindle

a | b | c

B

Egg Extract

0.3λ ———— 0.01λ

Depleted

kDa | M | 98

120
100 — Nup98
80
60
50
Rae1
40

1 2 3 4 5 6 7 8 9 10

C

mock depleted / Nup98 depleted

mock depleted + BSA / Nup98 depleted + BSA / Nup98 depleted + xenCterm / Nup98 depleted + huCterm

D

Treatment	Assay		
	Spindle assembly	Ran aster formation	Preformed spindles
Nup98 C-term addition	xs MT	xs MT	xs MT
Nup98 Ab addition	monopolar spindles	no effect	no effect
Nup98 depletion	monopolar spindles	+/- *	nd

Nup98 C-terminal domain interacts with the microtubule-depolymerizing kinesin MCAK

Addition of the Nup98 C-terminus in the absence of sperm chromatin or Ran-GTP did not result in spontaneous microtubule polymerization. This finding suggested that Nup98 could not initiate polymerization but more likely influenced microtubule dynamics. We initially tested the rate of microtubule flux using speckle microscopy (Waterman-Storer et al., 1999) but found that addition of the Nup98 C-terminus did not significantly alter the rate of flux (M. K. Cross, L. A. Cameron, E. D. Salmon, and M. A. Powers, unpublished data). We then considered a possible role for Nup98 in influencing plus-end microtubule dynamics, potentially through interaction with microtubule regulatory factors. One candidate regulatory protein is MCAK (Xenopus XKCM1), a depolymerizing kinesin of the KinI/kinesin-13 family and the major global regulator of microtubule catastrophe in the egg extract (Wordeman and Mitchison, 1995; Walczak et al., 1996; Desai et al., 1999b; Tournebize et al., 2000). Published studies have established that in the absence of MCAK, excess long microtubules are produced during spindle assembly, resulting in "hairy" spindles (Walczak et al., 1996; Mitchison et al., 2005). Conversely, increased MCAK activity inhibits bipolar spindle formation and results in monopolar spindles and asters (Ohi et al., 2004; Sampath et al., 2004). These phenotypes are the opposite of those observed following manipulation of Nup98, wherein excess C-terminus promotes long microtubule growth and depletion leads to an increase in monopolar spindles. Taken together, these data suggested that Nup98 might act as a negative regulator of MCAK activity during spindle formation.

To investigate this possibility, we performed pull-down experiments using purified Nup98 C-terminal fragments. Recombinant proteins were incubated in CSF extract to allow for binding and then recovered on beads, washed, and eluted. Antibody to the T7 tag was used for recovery to avoid potential competition between the Nup98 antibody and Nup98-binding proteins. Bound proteins were then immunoblotted using an antibody to the Xenopus MCAK homolog XKCM1 (Figure 5A). We detected association of MCAK with the longer Nup98 C-terminus (aa 506–920), but binding was greatly reduced with the shorter C-terminal domain (aa 678–920), which does not induce the excess microtubule phenotype. The mutant C-terminus (S864A), which also induced excess polymerization, bound MCAK at levels similar to the wild-type fragment.

Next, we asked whether we could detect interaction between endogenous Nup98 and MCAK proteins in the extract. Nup98 was immunoprecipitated from the CSF extract using an antibody directed toward the GLFG repeat domain to avoid possible competition with proteins binding the C-terminus (Figure 5B). We observed a small amount of MCAK coprecipitating with Nup98. Notably, our Nup98 depletion experiments did not codeplete MCAK from the extracts (Figure 5C). This is in keeping with the limited degree of coprecipitation of these proteins. Indeed, the phenotype of Nup98 and MCAK codepletion is distinct from what we observe following Nup98 depletion; codepletion resembles depletion of MCAK, in keeping with potential regulation of MCAK activity by Nup98 (Supplemental Figure 5).

The results thus far supported, but did not yet prove, a role for Nup98 as a regulator of MCAK function. To test this directly, we used an established in vitro depolymerization assay for measurement of MCAK activity (Desai and Walczak, 2001). Taxol-stabilized microtubules were formed in vitro from purified tubulin (the kind gift of Eric Griffis and Ron Vale, University of California, San Francisco) and isolated by centrifugation. After resuspension, microtubules were incubated for 20 min with purified MCAK (the kind gift of Stephanie Ems-McClure and Claire Walczak), intact microtubules were separated from released tubulin dimers by centrifugation, and equal fractions of pellet and supernatant were analyzed on gels. As expected, MCAK depolymerized microtubules in an ATP-dependent manner, leading to substantial reduction in the amount of pelleted tubulin (Figure 5D, top). When the full Nup98 C-terminal fragment (aa 506–920) was included in the assay, we noted a marked decrease in MCAK activity. In contrast, when either BSA or the shorter Nup98 fragment (aa 678–920) was added to the assay, MCAK activity was not altered. When we varied the concentration of both Nup98 C-terminal fragments in the in vitro depolymerization assay, we observed that the long but not the short fragment inhibited MCAK in a concentration-dependant manner (Supplemental Figure 6A). The amount of Nup98 C-terminus required for inhibition is well in excess of the amount of MCAK present in these assays; however, even at threefold higher concentration than shown, we saw no inhibitory affect on MCAK activity by the short fragment (unpublished data).

Nup98 interacts with microtubules to inhibit MCAK activity

Throughout the in vitro depolymerization assays, we noted a small but consistent amount of Nup98 cosedimented with microtubules. To test whether Nup98 might bind microtubules directly, we assembled the same assays in the absence of MCAK, leaving the microtubules intact. When microtubules were pelleted, the long C-terminal fragment cosedimented in a concentration-dependant manner. Far less of the short C-terminal fragment associated with the stabilized microtubules. Complementary results were obtained when the Nup98 fragments were recovered from the assays using the T7 tag; more tubulin was pulled down with the long C-terminal fragment (Supplemental Figure 6B).

It was possible that the Nup98–microtubule interaction could block MCAK from binding to microtubules, thereby preventing depolymerization. We therefore assembled the in vitro assays in the absence of ATP to allow MCAK to bind, but not depolymerize, microtubules. Under these conditions, we detected identical amounts

---

FIGURE 4: Depletion of Nup98 from Xenopus extracts causes disruption in bipolar spindle assembly, which can be restored by the Nup98 C-terminal domain. Extracts were depleted with either nonspecific IgG (mock) or anti-Nup98, and either BSA or purified Nup98 C-terminus was added to a final concentration of 1.5 μM. Spindles were assembled for 60 min. (A) Spindles assembled following Nup98 depletion and addback of the recombinant C-terminus. Microtubules are in red, and DNA is in blue. Scale bar is 20 μm. (B) Depletion was assessed by blotting 0.3 μl depleted extracts relative to serial twofold dilutions of Xenopus extract. (C) Spindle morphology was scored as bipolar, imperfect bipolar, or monopolar. Imperfect spindles typically resembled that of panel Ab, in which DNA was somewhat misaligned. Left, spindle morphology following mock depletion or depletion with anti-Nup98. Right, spindle morphology following depletion and addback of BSA or Nup98 C-terminus. Three or more independent experiments were scored for each condition, with 25–50 spindles per sample, for a total of 1429 spindles analyzed. Error bars represent SEP. (D) Summary of phenotypes observed after manipulation of Nup98 levels in Xenopus egg extract. *In depleted extracts, formation of Ran asters required an extra 15 min, but asters appeared normal. nd, not done.
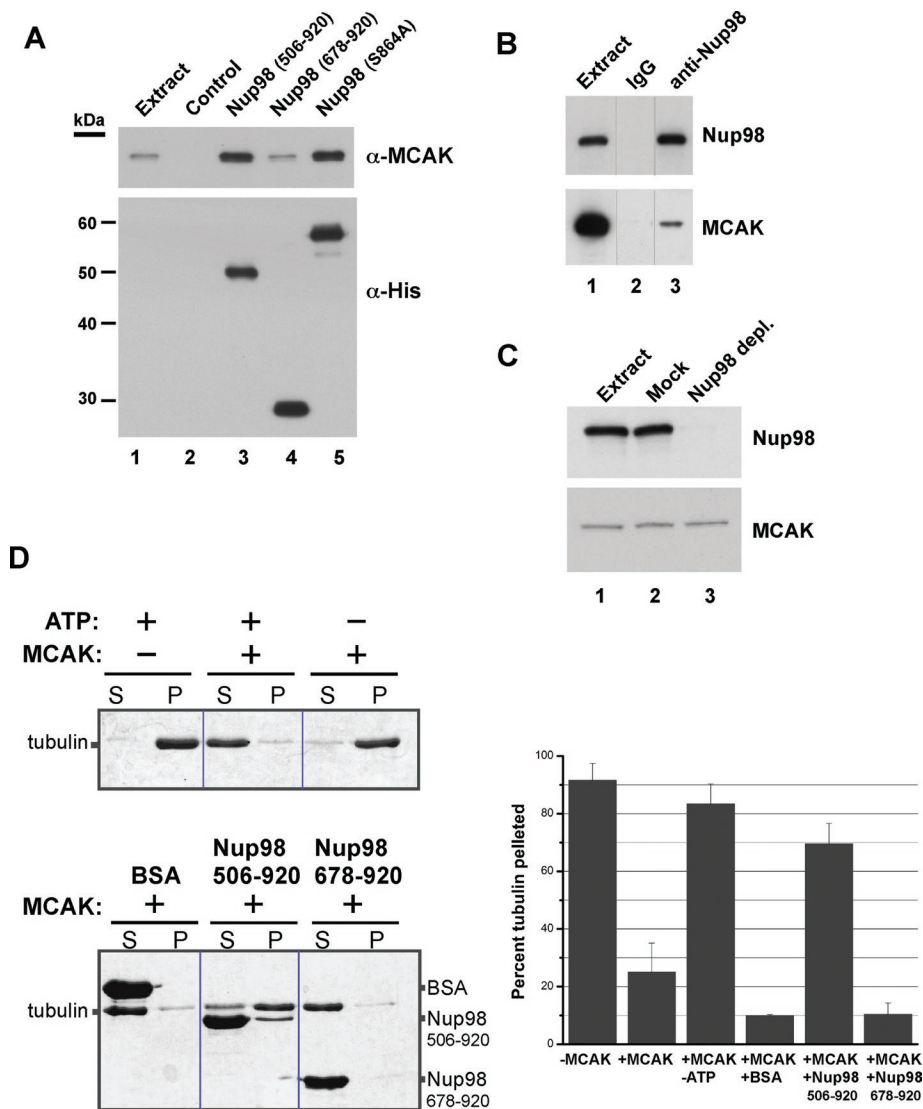
FIGURE 5: Nup98 interacts with MCAK through the C-terminal domain and can inhibit MCAK microtubule-depolymerizing activity in vitro. (A) Nup98 C-terminal fragments or buffer (control) were incubated with CSF extract, immunoprecipitated with anti-T7 antibodies, and immunoblotted with anti-XKCM1 (MCAK) or anti-His. Sample lanes contain the material isolated from 4 µl extract. Extract lane contains 0.1 µl extract. (B) Immunoprecipitations from CSF extract were performed with either control IgG or anti-Nup98 (αGLFG domain). IPs were immunoblotted with Nup98 antibody or anti-XKCM1. The Nup98 blot contains IP from 0.5 µl extract. The XKCM1 blot contains IP from 10 µl extract. The extract lane contains 0.1 µl extract. (C) Extracts were immunoblotted with either anti-Nup98 or anti-XKCM1 to determine the extent of XKCM1 codepleted. Each lane contains 0.2 µl extract. (D) In vitro MCAK microtubule depolymerization assays were performed, and equal fractions of the supernatant and pellet were run on PAGE and Coomassie stained. Left top, microtubule polymerization was dependent upon both MCAK and ATP. Left bottom, Nup98 aa 506–920, but not the shorter construct, inhibited microtubule depolymerization by MCAK. Right, microtubule-depolymerization activity is represented as % tubulin pelleted, calculated from spot densitometry of Coomassie-stained gels. Values represent the average of three independent experiments.

of MCAK cosedimenting with microtubules in the presence or absence of the Nup98 C-terminus (Supplemental Figure 6C). Thus Nup98 does not inhibit MCAK from binding to microtubules.

Finally, we investigated whether the Nup98 C-terminal domain could interact with MCAK directly. The pull-down experiments performed with egg extracts (Figure 5, A and B) do not distinguish between direct and indirect binding. Using concentrations of purified Nup98 C-terminus and MCAK that approximated those expected in

the diluted egg extract used for the earlier binding assays, we combined the purified recombinant proteins and recovered the Nup98 C-terminus using the T7 tag. We observed a small amount of MCAK binding to Nup98 C-terminal domain over controls, suggesting a potential but low affinity interaction between Nup98 and MCAK (Supplemental Figure 6D). Taken in sum, our data suggest that Nup98 acts to decrease MCAK-mediated depolymerization primarily through binding to microtubules and possibly through an additional weak interaction with MCAK directly.

DISCUSSION

Here we report a novel role for the nucleoporin Nup98 during mitosis. Use of the *X. laevis* egg extract system allowed us to explore potential mitotic function while circumventing effects of Nup98 perturbation on NPC structure or transport. Our findings indicate that Nup98 plays a role in the regulation of microtubule dynamics during spindle assembly in the extract. Addition of the Nup98 C-terminus promotes microtubule polymerization and, conversely, loss of Nup98 function leads to accumulation of monopolar spindles. These effects are the inverse of previously reported results following manipulation of the depolymerizing kinesin MCAK. We were able to demonstrate interaction between MCAK and the C-terminal domain of Nup98 in egg extracts and establish that the Nup98 C-terminus can inhibit MCAK microtubule depolymerization activity in vitro. Furthermore, the full Nup98 C-terminal domain can associate directly with microtubules. These findings led us to propose a model in which Nup98 binds to microtubules and opposes MCAK activity during spindle formation (Figure 6).

In the absence of Nup98, we see a substantial shift to half-spindles that are unable to progress to bipolar spindles. This result is highly reminiscent of the phenotype observed when MCAK regulation is lost through replacement of endogenous MCAK with a nonphosphorylatable mutant or through depletion of the CPC (Ohi *et al.*, 2004; Sampath *et al.*, 2004). The CPC is composed of four subunits: inner centromere protein (INCENP), Survivin, Dasra/Borealin, and the kinase Aurora B (reviewed in Ruchaud *et al.*, 2007). This multimeric complex is concentrated at the centromere and inhibits MCAK depolymerization activity through phosphorylation of MCAK at S196 (Andrews *et al.*, 2004; Lan *et al.*, 2004). In particular, we noted that our half-spindles strongly resemble those produced following depletion of Dasra A from *Xenopus* extracts (Sampath *et al.*, 2004). Dasra depletion codepletes ~70% of INCENP and Aurora B kinase; this leads to lack of MCAK phosphorylation, excess MCAK activity, and loss of spindle

A

B
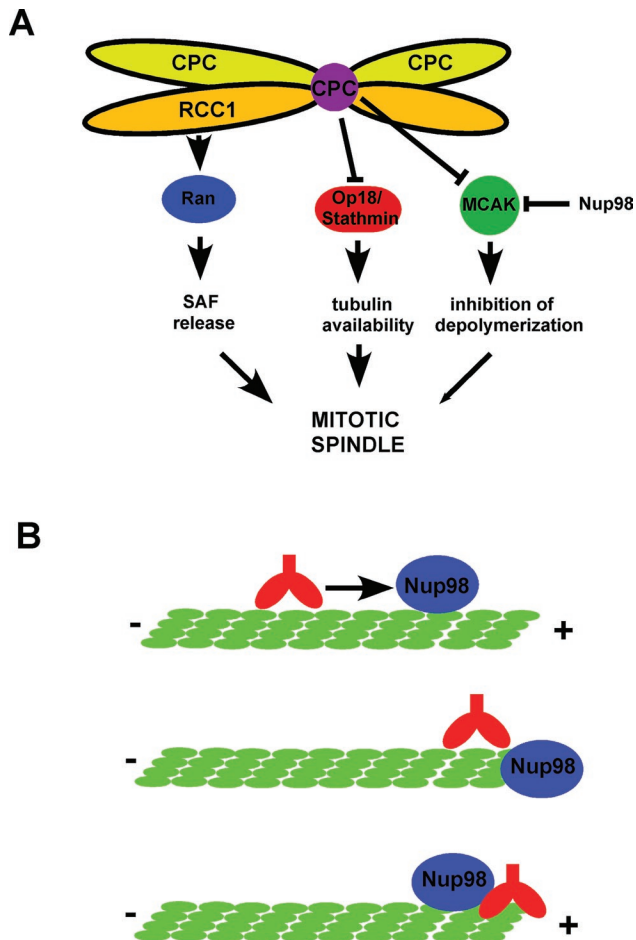
FIGURE 6: Model of Nup98 function in spindle assembly. (A) The Ran-GTP gradient generated by RCCI promotes spindle assembly factor release in the vicinity of chromatin. Bipolar spindle assembly also requires down-regulation of oncoprotein 18/stathmin and MCAK by the CPC. We propose that Nup98 also negatively regulates MCAK activity to promote bipolar spindle assembly. (B) Potential mechanisms for Nup98 regulation of MCAK function. Top, Nup98 binds to microtubules and prevents lateral diffusion of MCAK. Middle, Nup98 binds to microtubule plus ends and competes for MCAK binding and depolymerization of plus ends. Bottom, Nup98 binds microtubules and stabilizes them against MCAK depolymerization.

trast to the Nup98 depletion phenotype (Supplemental Figure 5). This is in keeping with our model that Nup98 serves as a check on MCAK activity; when MCAK is removed through depletion, removal of a regulatory protein should have no added or opposing affects.

Importantly, addition of the C-terminal domain to Nup98-depleted extract was sufficient to restore bipolar spindle formation, indicating that the Nup98 C-terminus can influence MCAK activity independently. In keeping with this, we found purified C-terminal domain to inhibit MCAK depolymerization activity in vitro. These findings support the model that the Nup98 C-terminus contains a domain responsible for promoting bipolar spindle assembly through regulation of microtubule depolymerization by MCAK. The region of Nup98 that lies between the unstructured nucleoporin repeats and the highly ordered autoproteolytic domain has not been previously linked to a specific function. We also find that this region is phosphorylated in *Xenopus* mitotic extracts, suggesting regulation by mitotic kinases, a possibility that is being further explored.

Regulation of MCAK by the CPC is thought to occur predominantly at the centromere/kinetochore. We were unable to detect Nup98 at the kinetochore, despite using three independent antibodies directed against full-length Nup98, the Nup98 C-terminus, or the Nup98 GLFG domain (Fukuhara *et al.*, 2005). Nonetheless, the formal possibility remains that there is a small but highly dynamic population of Nup98 transiently associated with the kinetochore that we are unable to detect. We recently reported that leukemogenic Nup98/Hox fusions, which contain the Nup98 GLFG domain but lack the C-terminus, are concentrated at kinetochores and chromosome arms during mitosis (Xu and Powers, 2010). This observation could represent stabilization by the DNA-binding Hox domain of an interaction that is highly transient with the wild-type Nup98 protein. This possibility remains to be further investigated.

We did observe that the full C-terminal domain of Nup98, to a much greater extent than the short C-terminal fragment, can bind to Taxol-stabilized microtubules in vitro. This finding raises the possibility that Nup98 could influence MCAK activity by acting as a microtubule-associated protein (MAP). This would be in keeping with the excess of Nup98 C-terminus required for inhibition of depolymerization, although it should be noted that endogenous nucleoporins are found at relatively high levels in the egg extract. Studies by others have shown that MCAK first binds laterally, on the side of the microtubule, and moves to the tip of the microtubule to depolymerize the polymer (Hunter *et al.*, 2003). Addition of the Nup98 C-terminus did not reduce the amount of MCAK associated with Taxol-stabilized microtubules; possibly Nup98 might interfere with MCAK movement to the microtubule plus end and thus prevent depolymerization; alternatively, Nup98 may interact with MCAK and other proteins at the plus end. Further studies to identify potential additional binding proteins, and to image Nup98 and MCAK interactions with microtubules, will be important to further discern the specific mechanism underlying the phenotypes we observe.

Nup98 can be isolated from high-speed supernatant of both interphase and mitotic egg extracts in a complex with Rae1 (Blevins *et al.*, 2003). In the crude CSF extracts, we found that only ~50% of Rae1 was codepleted with Nup98. Blower and colleagues (2005) previously described the association of Rae1 with a large multiprotein complex containing RNA-binding proteins as well as RNA. This complex plays an important role in spindle assembly and, further, may aid in partitioning critical transcripts encoding cell cycle and developmental regulators into daughter cells (Blower *et al.*, 2007). Nup98 was not directly shown to be present in this complex, and thus its contribution in this context is somewhat uncertain.

bipolarity. Similarly, depletion of MCAK followed by replacement with nonphosphorylatable, constitutively active MCAK mutants leads to formation of half-spindles (Ohi *et al.*, 2004). Both these results suggest that down-regulation of MCAK is required for spindle bipolarity although the underlying mechanisms leading to bipolarity in the extract are not entirely clear. More complete (~90%) depletion of the CPC using anti-INCENP resulted in chromatin with no associated microtubules (Sampath *et al.*, 2004). This is a phenotype that we saw only very rarely in our experiments, suggesting that loss of Nup98 does not leave MCAK without any check on its depolymerization activity.

In contrast to the monopolar spindles formed upon depletion or inactivation of Nup98, addition of excess C-terminal domain results in dysregulation of microtubule polymerization. Similar effects on microtubules are observed upon loss of MCAK activity (Walczak *et al.*, 1996; Ems-McClung *et al.*, 2007; Zhang *et al.*, 2008). When MCAK and Nup98 were codepleted from extract, we observed excess microtubules, as seen following MCAK depletion and in con-

Here we report a phenotype very distinct from that observed after depletion of Rae1 from the extract. Following Rae1 depletion (which was estimated to remove ~60–70% of the protein), spindle formation was strongly inhibited and only sparse, highly bundled microtubules were found (Blower *et al.*, 2005). This is in contrast to the monopolar spindles that we observe in Nup98 depletions. We did not find significant numbers of sperm chromatin without associated microtubules, nor did Nup98 depletion decrease the formation of Ran asters, as did Rae1 depletion. Addition of excess recombinant Rae1-binding domain, which competes with Nup98 for Rae1 binding (Blevins *et al.*, 2003), had no effect on spindle formation (Supplemental Figure 1), suggesting that interaction between these two is not essential for this process. Further, we saw no codepletion of another member of the Rae1 complex (Vera/VgRBP/Zbp1; Blower *et al.*, 2005) or a protein (CPEB) that interacts with components of the Rae1 complex (Maskin and cyclin B mRNA; Groisman *et al.*, 2000). Most importantly, following Nup98 depletion, we were able to restore spindle bipolarity with recombinant Nup98 C-terminus that lacks the Rae1-binding site. Taken together, we feel these results argue strongly for independent Nup98 and Rae1 roles in mitotic spindle assembly.

Recently the Nup107 complex was reported to interact with the γ-TuRC, a protein complex involved in microtubule nucleation, at the kinetochore. This interaction is thought to promote microtubule nucleation at the kinetochore, leading to stable K-fiber assembly (Mishra *et al.*, 2010). Thus it appears that nucleoporins play important regulatory roles in microtubule dynamics during mitosis when the pore is disassembled. Such contributions would ensure that a stable mitotic spindle does not form while the nuclear envelope and NPC are still intact. It seems likely that additional nucleoporins will continue to emerge as important regulators of mitosis.

MATERIALS AND METHODS
Preparation of *Xenopus* CSF extract and spindle assembly assay
CSF extract was prepared as described (Desai *et al.*, 1999a). To concentrate the extract, eggs were spun through 750 μl Nyosil oil (Nye Lubricants, Fairhaven, MA) before crushing. Demembranated sperm chromatin were isolated as described (Powers *et al.*, 2001). Spindle assembly assays were performed in CSF extract essentially as described (Desai *et al.*, 1999a). The extract was supplemented with 145 nM X-rhodamine tubulin (Cytoskeleton, Denver, CO) and sperm chromatin at 500/μl. Nup98 C-terminal fragment or BSA was added to 20 μl of this mix at a final concentration of 6 μM. For antibody addition, affinity-purified anti–human Nup98 C-terminal domain (Griffis *et al.*, 2002) was added at 200 μg/ml, and affinity-purified anti-*Xenopus* Nup98 C-terminus was added at 100 μg/ml. As a control, nonspecific Rb immunoglobulin G (IgG) (Calbiochem, La Jolla, CA) was used at equivalent concentrations. Assays were incubated at room temperature, and 2-μl aliquots were combined with 2 μl fix (60% glycerol, 1× MMR, 1 mg/ml Hoechst, 10% formaldehyde). Samples were analyzed using a BX60 microscope (Olympus, Tokyo, Japan) with either an 8-bit camera (Dage-MTI, Michigan City, IN) and IP Lab software (Scanalytics, Fairfax, VA) or a 16-bit camera (Hamamatsu, Bridgewater, NJ) and SlideBook software (Intelligent Imaging Innovations, Denver, CO). Antibody specificity controls were prepared by preincubating 4 μg antibody with ~2.5 μg purified Nup98 C-terminus before addition to the assay mix. Spindles were quantified as described in figure legends. Error bars are calculated as standard error of the mean or standard error of the proportion (SEP) using the equation $\sqrt{(P(1 - P)/n)}$, where P = percentage of sample and n = total number of spindles.

Tubulin spin-down assay
Tubulin spin-downs were performed as described (Budde *et al.*, 2001), with some modifications. The extract was supplemented with sperm chromatin at 5000/μl. Nup98 C-terminal fragment or BSA was added to 25 μl of this mix, and assays were incubated at room temperature for 30 min. Assays were diluted by triturating in 0.5 ml buffer (30% glycerol, 1× BRB80 [80 mM K-Pipes, pH 6.8, 1 mM MgCl$_2$, 1 mM ethylene glycol tetraacetic acid [EGTA], 1% Triton X-100) and layered onto a 1-ml cushion (40% glycerol, 1× BRB80). Polymerized tubulin was pelleted in a microcentrifuge for 10 min, RT. Tubulin pellets were resuspended in 200 μl gel sample buffer (SB). Two microliters of each sample were resolved on a 10% SDS–PAGE gel and immunoblotted for α-tubulin (Sigma-Aldrich, St. Louis, MO; 1:10,000), γ-tubulin (Sigma-Aldrich; 1:5000), or RCC1 (Mary S. Moore; 1:5000).

Depletions and protein addback
Depletions were performed as described (Desai *et al.*, 1999a) with some modifications. Antibodies were bound to Affi-prep protein A beads (BioRad, Hercules, CA) at 8 μg/25 μl beads, blocked, and washed as described. For depletions, 25 μl antibody-bound beads were rotated with 200 μl extract, 4°C, 30 min. The partially depleted extract was transferred to a fresh set of antibody beads and rotated for another 30 min. For protein addback experiments, only one 45-min depletion was used. Either BSA or Nup98 C-terminal fragment was added to the depleted extract at a concentration of 1.5 μM. For double depletions, 8 μg each of anti-xNup98 and anti-XKCM1 (MCAK) were bound to 25 μl Affi-prep protein A beads. Beads were incubated for 45 min with 200 μl CSF extract to deplete proteins, and the extent of depletion was analyzed by Western blotting.

Ran aster assay
Ran aster assays were performed as described (Wilde and Zheng, 1999) with some modifications. ZZ-RanQ69L (the kind gift of K. Weis, University of California, Berkeley) was added to *Xenopus* CSF extract at 25 μM. The extract was supplemented with X-rhodamine tubulin as above, and Nup98 C-terminus or BSA was added at a final concentration of 6 μM. Samples were fixed and analyzed as above.

Expression and purification of recombinant proteins
Nup98 C-terminal fragments, AA 505–920, AA 676–920, and AA 505–920 S864A, were subcloned into the pET 28a vector and expressed as N-terminal His-tagged proteins in *Escherichia coli* BL21(DE3) cells. Truncated Nup98 C-terminal fragments were generated by substitution of a stop codon for residues 668, 712, 775, or 864 by Stratagene QuikChange. The cells were grown to an OD$_{600}$ ~0.6 and induced with 0.5 mM isopropyl β-d-1-thiogalactopyranoside at 37°C for 3 h. The proteins were purified and dialyzed at 4°C into 20 mM HEPES (pH 7.5), 150 mM NaCl. Glycerol was added to 5%, and the protein was aliquoted, flash frozen, and stored at −80°C. His-ZZ-RanQ69L was expressed in *E. coli* M15 pREP cells, purified as above, and dialyzed into CSF-XB (10 mM K-HEPES [pH 7.7], 100 mM KCl, 2 mM MgCl$_2$, 0.1 mM CaCl$_2$, 50 mM sucrose, 5 mM EGTA).

IP of Nup98 from CSF extract
Antibodies were bound to Affi-prep protein A beads at 8 μg/25 μl beads. CSF extract (100 μl) was diluted to 1 ml with CSF-XB with protease inhibitors (10 mg/ml each leupeptin and chymostatin) and phosphatase inhibitors (5 mM NaPyrophosphate, 5 mM NaF, and

2 mM NaOrthovanadate). Diluted extract was briefly spun to remove large aggregates, and supernatant was precleared with protein A beads alone for 30 min at 4°C. Supernatant was added to beads containing either nonspecific rat IgG or Nup98 antibody targeted to the GLFG repeat domain. Samples were incubated for 1 h at 4°C. Beads were pelleted, washed four times in CSF-XB+PI+P'tase inhibitors, and eluted in 25 µl 2× SB.

Protein pull-downs from extract
Fifty microliters CSF extract was diluted to 1 ml in Tris-buffered saline containing 1% TX-100 (TBS-TX) + 20 mg/ml BSA, spun at 7500 × g, 4°C for 1 min, and the supernatant was incubated with 50 µl anti-T7 agarose at 4°C for 30 min with rotation to preclear. The anti-T7 beads were removed, and Nup98 fragments were added to the diluted extract and incubated at RT for 30 min with rotation. Samples were added to 50 µl anti-T7 agarose and were incubated at 4°C for 60 min with rotation. Beads were pelleted, washed four times in TBS-TX, washed once in TBS, and eluted in 50 µl 2× SB.

In vitro MCAK assay
In vitro MCAK assays were performed as described (Desai and Walczak, 2001) with minor alterations. Briefly, 100 µl reactions containing 1× BRB80, 1 mM dithiothreitol, 2 mM Mg-ATP, 25 nM MCAK, 2.5 mM KCl, 2 µM Taxol-stabilized MT, and 6 µM BSA or recombinant Nup98 C-terminal domain were mixed and incubated at room temperature for 20 min. Then 80 µl of each reaction was sedimented in an airfuge at ~90,000 rpm for 5 min at room temperature. The supernatant was collected, and the pellet was resuspended in 80 µl 1× BRB80, 5 mM $CaCl_2$, and 2.5 mM KCl. The resuspended pellet fraction was incubated on ice for 10 min, and the supernatant and pellet fractions were analyzed by SDS–PAGE and Coomassie stain.

Analysis of spindle area
Using MetaMorph software (Molecular Devices, Sunnyvale, CA), signals from X-rhodamine–labeled microtubules were thresholded to define the number of pixels per spindle or half-spindle. Pixels per square micron were determined using beads of defined size, and pixel areas were converted into square microns using this value.

REFERENCES
Andrews PD, Ovechkina Y, Morrice N, Wagenbach M, Duncan K, Wordeman L, Swedlow JR (2004). Aurora B regulates MCAK at the mitotic centromere. Dev Cell 6, 253–268.

Arnaoutov A, Dasso M (2005). Ran-GTP regulates kinetochore attachment in somatic cells. Cell Cycle 4, 1161–1165.

Belgareh N et al. (2001). An evolutionarily conserved NPC subcomplex, which redistributes in part to kinetochores in mammalian cells. J Cell Biol 154, 1147–1160.

Blevins MB, Smith AM, Phillips EM, Powers MA (2003). Complex formation among the RNA export proteins Nup98, Rae1/Gle2, and TAP. J Biol Chem 278, 20979–20988.

Blower MD, Feric E, Weis K, Heald R (2007). Genome-wide analysis demonstrates conserved localization of messenger RNAs to mitotic microtubules. J Cell Biol 179, 1365–1373.

Blower MD, Nachury M, Heald R, Weis K (2005). A Rae1-containing ribonucleoprotein complex is required for mitotic spindle assembly. Cell 121, 223–234.

Budde PP, Kumagai A, Dunphy WG, Heald R (2001). Regulation of op18 during spindle assembly in Xenopus egg extracts. J Cell Biol 153, 149–158.

Capelson M, Liang Y, Schulte R, Mair W, Wagner U, Hetzer MW (2010). Chromatin-bound nuclear pore components regulate gene expression in higher eukaryotes. Cell 140, 372–383.

Carazo-Salas RE, Guarguaglini G, Gruss OJ, Segref A, Karsenti E, Mattaj IW (1999). Generation of GTP-bound Ran by RCC1 is required for chromatin-induced mitotic spindle formation. Nature 400, 178–181.

Clarke PR, Zhang C (2008). Spatial and temporal coordination of mitosis by Ran GTPase. Nat Rev Mol Cell Biol 9, 464–477.

D'Angelo MA, Hetzer MW (2008). Structure, dynamics and function of nuclear pore complexes. Trends Cell Biol 18, 456–466.

Desai A, Murray A, Mitchison TJ, Walczak CE (1999a). The use of Xenopus egg extracts to study mitotic spindle assembly and function in vitro. Methods Cell Biol 61, 385–412.

Desai A, Verma S, Mitchison TJ, Walczak CE (1999b). Kin I kinesins are microtubule-destabilizing enzymes. Cell 96, 69–78.

Desai A, Walczak CE (2001). Assays for microtubule-destabilizing kinesins. Methods Mol Biol 164, 109–121.

Devos D, Dokudovskaya S, Williams R, Alber F, Eswar N, Chait BT, Rout MP, Sali A (2006). Simple fold composition and modular architecture of the nuclear pore complex. Proc Natl Acad Sci USA 103, 2172–2177.

Ems-McClung SC, Hertzer KM, Zhang X, Miller MW, Walczak CE (2007). The interplay of the N- and C-terminal domains of MCAK control microtubule depolymerization activity and spindle assembly. Mol Biol Cell 18, 282–294.

Fontoura BM, Blobel G, Yaseen NR (2000). The nucleoporin Nup98 is a site for GDP/GTP exchange on Ran and termination of karyopherin β2-mediated nuclear import. J Biol Chem 275, 31289–31296.

Franz C, Walczak R, Yavuz S, Santarella R, Gentzel M, Askjaer P, Galy V, Hetzer M, Mattaj IW, Antonin W (2007). MEL-28/ELYS is required for the recruitment of nucleoporins to chromatin and postmitotic nuclear pore complex assembly. EMBO Rep 8, 165–172.

Fukuhara T, Ozaki T, Shikata K, Katahira J, Yoneda Y, Ogino K, Tachibana T (2005). Specific monoclonal antibody against the nuclear pore complex protein, Nup98. Hybridoma 24, 244–247.

Griffis ER, Altan N, Lippincott-Schwartz J, Powers MA (2002). Nup98 is a mobile nucleoporin with transcription-dependent dynamics. Mol Biol Cell 13, 1282–1297.

Griffis ER, Xu S, Powers MA (2003). Nup98 localizes to both nuclear and cytoplasmic sides of the nuclear pore and binds to two distinct nucleoporin subcomplexes. Mol Biol Cell 14, 600–610.

Groisman I, Huang YS, Mendez R, Cao Q, Theurkauf W, Richter JD (2000). CPEB, maskin, and cyclin B1 mRNA at the mitotic apparatus: implications for local translational control of cell division. Cell 103, 435–447.

Gruss OJ, Carazo-Salas RE, Schatz CA, Guarguaglini G, Kast J, Wilm M, Le Bot N, Vernos I, Karsenti E, Mattaj IW (2001). Ran induces spindle assembly by reversing the inhibitory effect of importin α on TPX2 activity. Cell 104, 83–93.

Hodel A, Hodel M, Griffis E, Hennig K, Ratner G, Xu S, Powers M (2002). The three-dimensional structure of the autoproteolytic, nuclear pore-targeting domain of the human nucleoporin Nup98. Mol Cell 10, 347–358.

Hunter AW, Caplow M, Coy DL, Hancock WO, Diez S, Wordeman L, Howard J (2003). The kinesin-related protein MCAK is a microtubule depolymerase that forms an ATP-hydrolyzing complex at microtubule ends. Mol Cell 11, 445–457.

Jeganathan KB, Malureanu L, van Deursen JM (2005). The Rae1–Nup98 complex prevents aneuploidy by inhibiting securin degradation. Nature 438, 1036–1039.

Joseph J, Liu ST, Jablonski SA, Yen TJ, Dasso M (2004). The RanGAP1-RanBP2 complex is essential for microtubule-kinetochore interactions in vivo. Curr Biol 14, 611–617.

Joseph J, Tan SH, Karpova TS, McNally JG, Dasso M (2002). SUMO-1 targets RanGAP1 to kinetochores and mitotic spindles. J Cell Biol 156, 595–602.

Kalab P, Heald R (2008). The RanGTP gradient—a GPS for the mitotic spindle. J Cell Sci 121, 1577–1586.

Kalab P, Pu RT, Dasso M (1999). The Ran GTPase regulates mitotic spindle assembly. Curr Biol 9, 481–484.

Kalverda B, Pickersgill H, Shloma VV, Fornerod M (2010). Nucleoporins directly stimulate expression of developmental and cell-cycle genes inside the nucleoplasm. Cell 140, 360–371.

Knauer SK, Bier C, Habtemichael N, Stauber RH (2006). The Survivin–Crm1 interaction is essential for chromosomal passenger complex localization and function. EMBO Rep 7, 1259–1265.

Koffa MD, Casanova CM, Santarella R, Kocher T, Wilm M, Mattaj IW (2006). HURP is part of a Ran-dependent complex involved in spindle formation. Curr Biol 16, 743–754.

Kutay U, Hetzer MW (2008). Reorganization of the nuclear envelope during open mitosis. Curr Opin Cell Biol 20, 669–677.

Lan W, Zhang X, Kline-Smith SL, Rosasco SE, Barrett-Wilt GA, Shabanowitz J, Hunt DF, Walczak CE, Stukenberg PT (2004). Aurora B phosphorylates centromeric MCAK and regulates its localization and microtubule depolymerization activity. Curr Biol 14, 273–286.

Lee SH, Sterling H, Burlingame A, McCormick F (2008). Tpr directly binds to Mad1 and Mad2 and is important for the Mad1–Mad2-mediated mitotic spindle checkpoint. Genes Dev 22, 2926–2931.

Loiodice I, Alves A, Rabut G, Van Overbeek M, Ellenberg J, Sibarita JB, Doye V (2004). The entire Nup107–160 complex, including three new members, is targeted as one entity to kinetochores in mitosis. Mol Biol Cell 15, 3333–3344.

Lussi YC, Shumaker DK, Shimi T, Fahrenkrog B (2010). The nucleoporin Nup153 affects spindle checkpoint activity due to an association with Mad1. Nucleus 1, 71–84.

Mackay DR, Elgort SW, Ullman KS (2009). The nucleoporin Nup153 has separable roles in both early mitotic progression and the resolution of mitosis. Mol Biol Cell 20, 1652–1660.

Maresca TJ, Niederstrasser H, Weis K, Heald R (2005). Xnf7 contributes to spindle integrity through its microtubule-bundling activity. Curr Biol 15, 1755–1761.

Mishra RK, Chakraborty P, Arnaoutov A, Fontoura BM, Dasso M (2010). The Nup107–160 complex and γ-TuRC regulate microtubule polymerization at kinetochores. Nat Cell Biol 12, 164–169.

Mitchison TJ, Maddox P, Gaetz J, Groen A, Shirasu M, Desai A, Salmon ED, Kapoor TM (2005). Roles of polymerization dynamics, opposed motors, and a tensile element in governing the length of Xenopus extract meiotic spindles. Mol Biol Cell 16, 3064–3076.

Nachury MV, Maresca TJ, Salmon WC, Waterman-Storer CM, Heald R, Weis K (2001). Importin β is a mitotic target of the small GTPase Ran in spindle assembly. Cell 104, 95–106.

O'Brien LL, Albee AJ, Liu L, Tao W, Dobrzyn P, Lizarraga SB, Wiese C (2005). The Xenopus TACC homologue, maskin, functions in mitotic spindle assembly. Mol Biol Cell 16, 2836–2847.

O'Connell CB, Khodjakov AL (2007). Cooperative mechanisms of mitotic spindle formation. J Cell Sci 120, 1717–1722.

Ohba T, Nakamura M, Nishitani H, Nishimoto T (1999). Self-organization of microtubule asters induced in Xenopus egg extracts by GTP-bound Ran. Science 284, 1356–1358.

Ohi R, Sapra T, Howard J, Mitchison TJ (2004). Differentiation of cytoplasmic and meiotic spindle assembly MCAK functions by Aurora B-dependent phosphorylation. Mol Biol Cell 15, 2895–2906.

Orjalo AV, Arnaoutov A, Shen Z, Boyarchuk Y, Zeitlin SG, Fontoura B, Briggs S, Dasso M, Forbes DJ (2006). The Nup107–160 nucleoporin complex is required for correct bipolar spindle assembly. Mol Biol Cell 17, 3806–3818.

Platani M, Santarella-Mellwig R, Posch M, Walczak R, Swedlow JR, Mattaj IW (2009). The Nup107–160 nucleoporin complex promotes mitotic events via control of the localization state of the chromosome passenger complex. Mol Biol Cell 20, 5260–5275.

Powers M, Evans EK, Yang J, Kornbluth S (2001). Preparation and use of interphase Xenopus egg extracts. Curr Protoc Cell Biol 11.10.1–11.1.24.

Powers MA, Forbes DJ, Dahlberg JE, Lund E (1997). The vertebrate GLFG nucleoporin, Nup98, is an essential component of multiple RNA export pathways. J Cell Biol 136, 241–250.

Powers MA, Macaulay C, Masiarz FR, Forbes DJ (1995). Reconstituted nuclei depleted of a vertebrate GLFG nuclear pore protein, p97, import but are defective in nuclear growth and replication. J Cell Biol 128, 721–736.

Rabut G, Lenart P, Ellenberg J (2004). Dynamics of nuclear pore complex organization through the cell cycle. Curr Opin Cell Biol 16, 314–321.

Radu A, Moore MS, Blobel G (1995). The peptide repeat domain of nucleoporin Nup98 functions as a docking site in transport across the nuclear pore complex. Cell 81, 215–222.

Raemaekers T, Ribbeck K, Beaudouin J, Annaert W, Van Camp M, Stockmans I, Smets N, Bouillon R, Ellenberg J, Carmeliet G (2003). NuSAP, a novel microtubule-associated protein involved in mitotic spindle organization. J Cell Biol 162, 1017–1029.

Rasala BA, Orjalo AV, Shen Z, Briggs S, Forbes DJ (2006). ELYS is a dual nucleoporin/kinetochore protein required for nuclear pore assembly and proper cell division. Proc Natl Acad Sci USA 103, 17801–17806.

Robinson MA, Park S, Sun ZY, Silver PA, Wagner G, Hogle JM (2005). Multiple conformations in the ligand-binding site of the yeast nuclear pore-targeting domain of Nup116p. J Biol Chem 280, 35723–35732.

Rosenblum JS, Blobel G (1999). Autoproteolysis in nucleoporin biogenesis. Proc Natl Acad Sci USA 96, 11370–11375.

Roux KJ, Burke B (2006). From pore to kinetochore and back: regulating envelope assembly. Dev Cell 11, 276–278.

Ruchaud S, Carmena M, Earnshaw WC (2007). Chromosomal passengers: conducting cell division. Nat Rev Mol Cell Biol 8, 798–812.

Salina D, Enarson P, Rattner JB, Burke B (2003). Nup358 integrates nuclear envelope breakdown with kinetochore assembly. J Cell Biol 162, 991–1001.

Sampath SC, Ohi R, Leismann O, Salic A, Pozniakovski A, Funabiki H (2004). The chromosomal passenger complex is required for chromatin-induced microtubule stabilization and spindle assembly. Cell 118, 187–202.

Schwartz TU (2005). Modularity within the architecture of the nuclear pore complex. Curr Opin Struct Biol 15, 221–226.

Terry LJ, Shows EB, Wente SR (2007). Crossing the nuclear envelope: hierarchical regulation of nucleocytoplasmic transport. Science 318, 1412–1416.

Tournebize R, Popov A, Kinoshita K, Ashford AJ, Rybina S, Pozniakovsky A, Mayer TU, Walczak CE, Karsenti E, Hyman AA (2000). Control of microtubule dynamics by the antagonistic activities of XMAP215 and XKCM1 in Xenopus egg extracts. Nat Cell Biol 2, 13–19.

Tran EJ, Wente SR (2006). Dynamic nuclear pore complexes: life on the edge. Cell 125, 1041–1053.

Vasu S, Shah S, Orjalo A, Park M, Fischer WH, Forbes DJ (2001). Novel vertebrate nucleoporins Nup133 and Nup160 play a role in mRNA export. J Cell Biol 155, 339–354.

Walczak CE, Heald R (2008). Mechanisms of mitotic spindle assembly and function. Int Rev Cytol 265, 111–158.

Walczak CE, Mitchison TJ, Desai A (1996). XKCM1: a Xenopus kinesin-related protein that regulates microtubule dynamics during mitotic spindle assembly. Cell 84, 37–47.

Waterman-Storer C, Desai A, Salmon ED (1999). Fluorescent speckle microscopy of spindle microtubule assembly and motility in living cells. Methods Cell Biol 61, 155–173.

Whalen WA, Bharathi A, Danielewicz D, Dhar R (1997). Advancement through mitosis requires rae1 gene function in fission yeast. Yeast 13, 1167–1179.

Wiese C, Wilde A, Moore MS, Adam SA, Merdes A, Zheng Y (2001). Role of importin-β in coupling Ran to downstream targets in microtubule assembly. Science 291, 653–656.

Wilde A, Zheng Y (1999). Stimulation of microtubule aster formation and spindle assembly by the small GTPase Ran. Science 284, 1359–1362.

Wong RW, Blobel G, Coutavas E (2006). Rae1 interaction with NuMA is required for bipolar spindle formation. Proc Natl Acad Sci USA 103, 19783–19787.

Wordeman L, Mitchison TJ (1995). Identification and partial characterization of mitotic centromere-associated kinesin, a kinesin-related protein that associates with centromeres during mitosis. J Cell Biol 128, 95–104.

Xu S, Powers MA (2010). Nup98-homeodomain fusions interact with endogenous Nup98 during interphase and localize to kinetochores and chromosome arms during mitosis. Mol Biol Cell 21, 1585–1596.

Zhang C, Hughes M, Clarke PR (1999). Ran-GTP stabilises microtubule asters and inhibits nuclear assembly in Xenopus egg extracts. J Cell Sci 112, 2453–2461.

Zhang X, Ems-McClung SC, Walczak CE (2008). Aurora A phosphorylates MCAK to control Ran-dependent spindle bipolarity. Mol Biol Cell 19, 2752–2765.

Zuccolo M et al. (2007). The human Nup107–160 nuclear pore subcomplex contributes to proper kinetochore functions. EMBO J 26, 1853–1864.